Paramagnetic defect centres in crystalline Alq_3

2005 J. Phys.: Condens. Matter 17 6271

(http://iopscience.iop.org/0953-8984/17/39/012)

INSTITUTE OF PHYSICS PUBLISHING JOURNAL OF PHYSICS: CONDENSED MATTER

J. Phys.: Condens. Matter **17** (2005) 6271–6283 doi:10.1088/0953-8984/17/39/012

Paramagnetic defect centres in crystalline Alq_3

M N Grecu[1,4], A Mirea[2], C Ghica[1], M Cölle[3] and M Schwoerer[2]

[1] National Institute for Materials Physics, POB MG-7, 077125 Magurele-Bucharest, Romania
[2] Experimental Physics II, Bayreuth University, 95440 Bayreuth, Germany
[3] Philips Research, Laboratories, NL-5656 AA Eindhoven, The Netherlands

E-mail: mgrecu@infim.ro

Received 12 May 2005, in final form 4 August 2005
Published 16 September 2005
Online at stacks.iop.org/JPhysCM/17/6271

Abstract

X- and Q-band electron paramagnetic resonance (EPR) investigation of different crystalline Alq_3 (tris(8-hydroxyquinoline)aluminium (III)) fractions formed by a train sublimation method are reported. Several paramagnetic defect centres corresponding to $1/2$, 1, and $3/2$ spin are observed at room temperature. Their intensity is dependent on the temperature, nature of the crystalline phase, and preparation conditions. Spectra simulation and analysis based on the spin Hamiltonian appropriate to a high spin system ($S \geqslant 1$) suggest the existence of randomly oriented triplets and quartets in annealed Alq_3 fractions. The crystalline Alq_3 phases responsible for the EPR powder spectra have been identified by transmission electron microscopy measurements performed on these sample fractions.

(Some figures in this article are in colour only in the electronic version)

1. Introduction

Since the discovery in 1987 [1] of its electroluminescent properties, Alq_3 (tris(8-hydroxyquinoline)aluminium (III)) has become one of the most used materials in organic light emitting devices (OLEDs) [2]. Much research has been carried out aimed at improving its light emission quantum efficiency and time stability. In spite of this, many fundamental questions concerning its properties, their dependence on thermal and annealing treatments, and its crystalline structure remain unanswered. Several experimental physical techniques (x-ray powder diffraction [3–5], optical spectroscopy and luminescence [6–10], Raman and infrared spectroscopy [11–13], NMR [14–16], ESR [17–19]) and theoretical methods of bonding analysis and reactivity [20, 21] have been used to study the crystalline state of Alq_3. Recently a significant blue shifted luminescence of a new phase (the so-called δ-phase) has been reported [10], increasing even further the interest in this material.

[4] Author to whom any correspondence should be addressed.

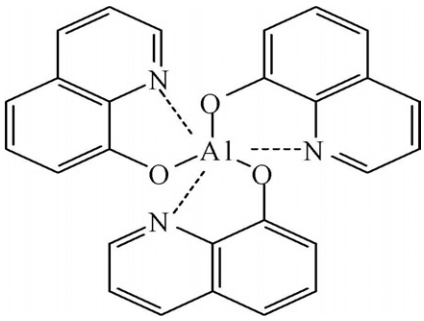

Figure 1. Chemical structure of the Alq_3 ($C_{27}H_{18}AlN_3O_3$) molecule.

Alq_3 is an octahedrally coordinated chelate complex, where the aluminium ion is surrounded by three identical quinolinolate anions (see figure 1). The two geometric isomers, meridianal (mer-Alq_3) and facial (fac-Alq_3), have C_1 and C_3 symmetry respectively [20, 22]. In principle, the two isomers could coexist, although mer-Alq_3 is energetically more stable than fac-Alq_3 by 4–7 kcal mol^{-1} [22]. Until recently, only the meridianal isomer was clearly identified in the α- and β-Alq_3 phases [3]. Recent x-ray structural analysis [5], optical measurements [4, 6], vibrational analysis [13], and NMR investigations [14] have proved that the newly discovered high temperature δ-Alq_3 phase consists of the facial isomer of the Alq_3 molecule.

It is well known that the performance of OLEDs depends on various factors including bulk properties of the organic material. Among the bulk properties, the local structural properties, the carrier mobility, and the stability are very important as they influence the efficiency and lifetime of the device. In order, therefore, to analyse local structural and electronic properties of Alq_3 crystalline phases in more detail, we performed electron paramagnetic resonance (EPR) investigations. To date three EPR investigations have been reported. Ravi Kishore *et al* [18] reported on the existence of a negative ion of Alq_3 in solution and thin film, which is paramagnetic with an effective paramagnetic moment of 0.9 μ_B per Alq^-. However, they could not detect any EPR signal even at low temperatures. On the other hand, the existence of a very weak EPR signal for yellow Alq_3 powder that is sensitive to γ-irradiation was communicated in [17]. This was attributed to organic free radicals by Roy *et al* [19].

In the present paper we report on the first X- and Q-band EPR measurements carried out in a large temperature range, 10–600 K, on sublimated solid Alq_3. Further attention is devoted to the discussion concerning the effect of annealing the crystalline Alq_3 fractions in an inert atmosphere, and of irradiation with an accelerated electron beam. The EPR results are correlated with transmission electron microscopy (TEM) measurements performed on the same Alq_3 samples.

2. Experimental details

Polycrystalline powders of different phases of Alq_3 were obtained by sublimation in a horizontal glass tube with a temperature gradient (320–380 °C), or by direct annealing of the powder at a defined temperature, in an inert atmosphere as described in [10, 23]. The formation of the crystalline phases obtained is temperature dependent. In the glass tube three main fractions (1, 2, and 3) of different crystalline phases of Alq_3 were distinguished, which are stable at room temperature. For some of our experiments we further distinguished six zones,

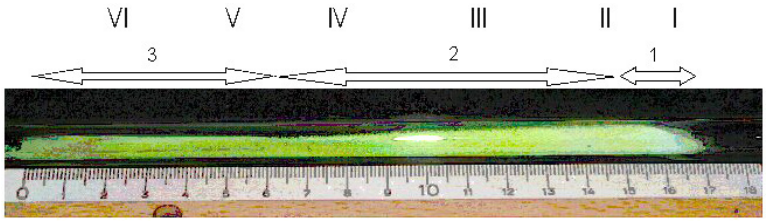

Figure 2. Picture of a sublimation tube. The three main fractions 1, 2, 3 correspond to the blue, yellow, and green crystalline Alq_3, respectively. The positions labelled I–VI correspond to the selected samples.

labelled I to VI, as shown in figure 2. Fraction 1 (a whitish microcrystalline powder with blue fluorescence) is the smallest amount formed at the hottest zone. Fraction 2, composed of yellowish acicular microcrystalline grains with green–yellow fluorescence, is the main fraction in the middle zone of the tube. Fraction 3, formed in the coldest zone, contains small green crystals of different morphologies with green fluorescence.

The EPR measurements were performed using an X-band JEOL JES-ME upgrade spectrometer, equipped with a JEOL system for low and high temperature experiments (100–570 K), and a Bruker ESP-300E spectrometer, at the Q band, where the temperature was controlled in the range 10–300 K using an Oxford Instruments ESR-900 continuous-flow helium cryostat. EPR spectra were recorded from 10 to 550 K, on Alq_3 samples prepared as follows: (a) as taken from the tube, (b) treated at different annealing temperatures (between 390 and 400 °C), and (c) exposed to high energy electron irradiation at room temperature (the irradiation dose was 10 kGy).

The TEM measurements were performed with a JEOL 200CX electron microscope operated at 200 kV. TEM specimens were prepared by fine grinding of the powder product and collecting crystal grains on TEM grids covered with holey membranes. It is important to note that no crystalline phase transitions were noticed during the observation of the samples in the TEM, including selected area electron diffraction (SAED) pattern recording.

3. EPR and TEM results

For the neutral and undisturbed Alq_3 molecule no EPR signal is expected, but for all samples investigated we obtained an EPR spectrum, depending on the sample treatment and preparation conditions. In the following we present in detail the features of these EPR signals for different Alq_3 fractions with the different crystalline phases, as identified by transmission electron microscopy.

3.1. Structural information—TEM measurements

From x-ray powder diffraction measurements, fractions 2 and 3 are similar, with a triclinic symmetry (SG $P\bar{1}$) and lattice parameters $a = 6.27$ Å, $b = 12.91$ Å, $c = 14.73$ Å; $\alpha = 109.6°$, $\beta = 89.7°$, $\gamma = 97.7°$, and $V = 1110$ Å^3 [4]. They correspond to α-Alq_3 phase. The crystal structure data for fraction 1, called the δ-Alq_3 phase and recently published [5, 10], also has a triclinic symmetry, but different cell parameters: $a = 13.241$ Å, $b = 14.424$ Å, $c = 6.177$ Å; $\alpha = 88.5°$, $\beta = 95.92°$, $\gamma = 113.93°$, and $V = 1072.38$ Å^3. Another high temperature phase, namely γ-Alq_3, has a trigonal symmetry (SG $P\bar{3}1c$) with lattice parameters of $a = b = 14.41$ Å, $c = 6.22$ Å, $\alpha = \beta = 90°$, $\gamma = 120°$ [4].

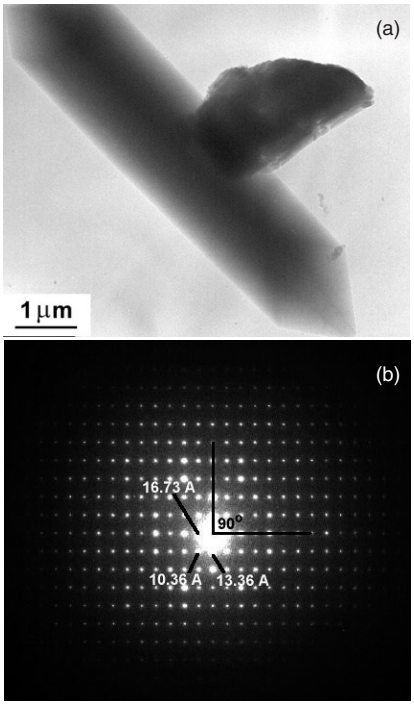

Figure 3. Needle-like crystal grain (a) and the corresponding SAED pattern (b), revealing the presence of a new unknown crystallographic phase. The 16.73 Å interplanar distance is not characteristic of any of the known Alq_3 phases. The 90° angle on the SAED pattern indicates a crystallographic system with a symmetry that is higher than triclinic.

From the electron diffraction point of view, where individual grains can be selected for TEM measurements, all selected fractions for the EPR measurements are a mixture of different crystalline Alq_3 phases, according to SAED patterns. Thus, the powder from fraction 1 is a complex mixture of δ- and γ-Alq_3 phases and a new Alq_3 phase not yet indexed according to any well known crystalline phases. The powder samples of fraction 3 prove to be a mixture of α-Alq_3 and the new, not yet specified, crystalline phase. An example of a SAED pattern of an oriented grain belonging to this crystalline phase in fraction 3 is given in figure 3. We note that the needle-like crystals of this phase, having a length of about 1.5–2 μm and a width around 0.3 μm, are mainly seen in fraction 2 and are present in the annealed Alq_3 fractions as well. The 90° angle found on the SAED pattern seen in figure 3 indicates for this new phase a crystallographic system with a symmetry higher than triclinic. None of the SAED patterns recorded for individual oriented grains in all fractions could be indexed according to the β-Alq_3 crystalline phase.

In the samples of fractions 2 and 3, after annealing for two hours in an inert atmosphere, the dimensions of grains are much smaller and the powder is generally a mixture of α-, γ-Alq_3 phases and the new unspecified crystalline phase dependent on the annealing temperature in the range 390–400 °C. On increasing the time of annealing up to 6 h only γ- and δ-Alq_3 phases were identified. Morphologically, the TEM images present crystallites of various irregular shapes with sizes from tens of nanometres to a few micrometres long, as resulted from TEM specimen preparation. Besides these small crystal grains, one can also note the presence of long needle grains, about 0.5 μm wide and up to a few micrometres long. Another interesting result was

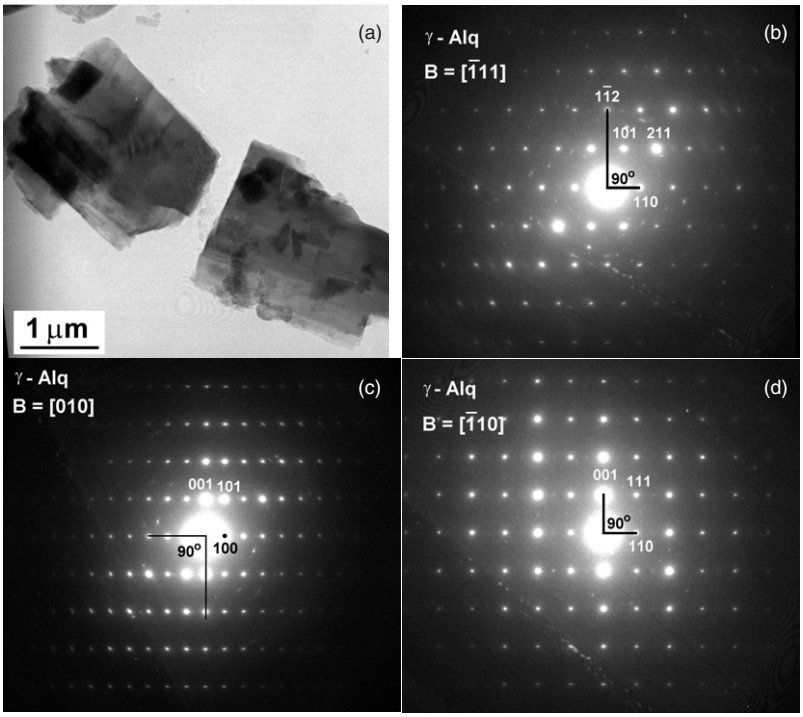

Figure 4. (a) TEM image of typical micrometric grains showing cleavage steps. (b) Single-crystal SAED pattern of a grain oriented close to the trigonal [$\bar{1}$11] zone axis. (c) Single-crystal SAED pattern of a grain oriented close to the trigonal [010] zone axis. (d) Single-crystal SAED pattern of a grain oriented close to the trigonal [1$\bar{1}$0] zone axis.

obtained for an annealed fraction 2 suddenly quenched at 77 K. In this case, all single-crystal SAED patterns recorded for individual grains were indexed according to the γ-Alq_3 phase only. In figures 4(a)–(d) we present a typical TEM image of large micrometric crystal grains showing cleavage steps (figure 4(a)) and single-crystal SAED patterns recorded for different such grains oriented along three principal zone axes (figures 4(b)–(d)). It has been shown that the ratio between δ- and γ-Alq_3 is strongly dependent on the preparation conditions [23]. As the recorded SAED patterns were indexable according to the γ-Alq_3 phase, we consider that this sample of fraction 2, annealed at 400 °C and quenched at 77 K, mainly consists of the trigonal crystalline phase. More detailed information about TEM measurements on Alq_3 phases will be given in [24].

3.2. EPR on microcrystalline Alq_3 as synthesized

Six samples, I to VI, selected from six zones along the sublimation tube (see figure 2) have been measured in the X band (9.5 GHz) and Q band (34 GHz). Typical EPR spectra are given in figure 5(a); it shows two types of signal, here labelled A and B, that are centred in the $g = 2$ and 4 regions of the spectrum in the X band, respectively. Their intensity I_{DI}, obtained by double integration, is dependent on the sample position in the glass tube, i.e. on the temperature of preparation. In figure 5(b), the position dependence of the EPR signal intensities of the six Alq_3 samples is shown. All samples consisted of 20 mg powder that was taken from the appropriate position of the sublimation tube. It is observed that the spectra

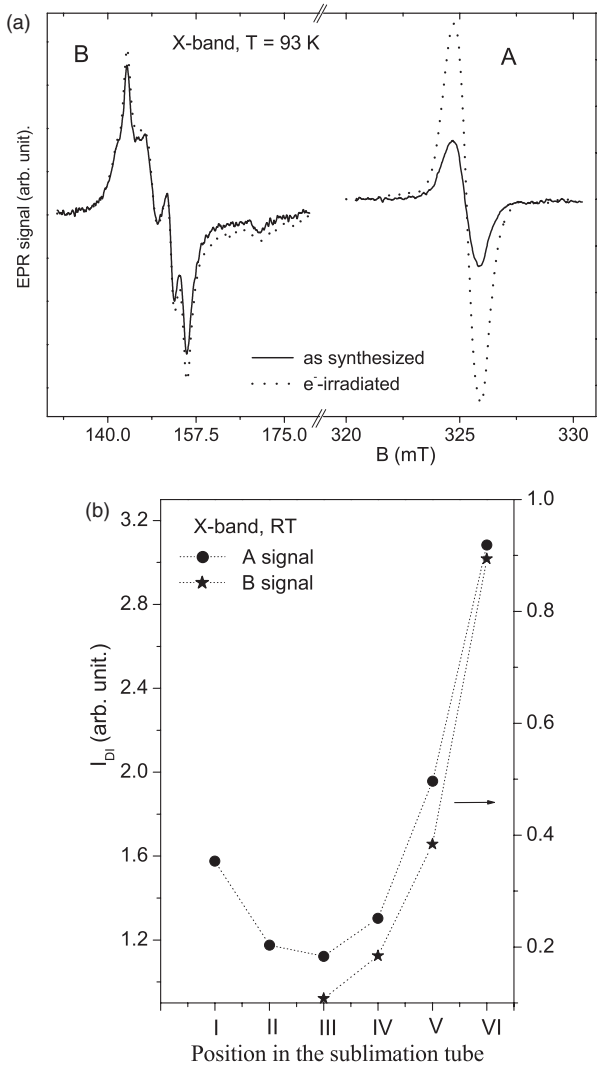

Figure 5. (a) Typical EPR spectra in the X band at 93 K for Alq_3 as synthesized and e^- irradiated. (b) Room temperature line intensity dependence of the A and B signals along the sublimation tube. The dotted line is a guide for the eye.

of samples V and VI (fraction 3), taken from the coldest zone of the tube have the highest intensities for both signals. The main spectral characteristics of these signals, the g values and the linewidths ΔB_{pp}, are given in table 1.

In the Q band, signal A has a resolved anisotropic g-tensor with two distinct values, $g_1 = 2.0040$ and $g_2 = g_3 = 2.0015$ (similarly to an axial symmetry centre). The signals observed around $g_{eff} = 4.3$ are weak, and clearly seen at low temperatures even for fractions 1 and 2. Both the A and B signals were measured at different temperatures. The inset in figure 6 shows the temperature dependence of these signals in the region 100–290 K. Signal B, which for samples of fraction 3 is structured at low temperature, behaves like that of a normal paramagnetic centre; its intensity increases linearly with $1/T$. On the other hand, signal A,

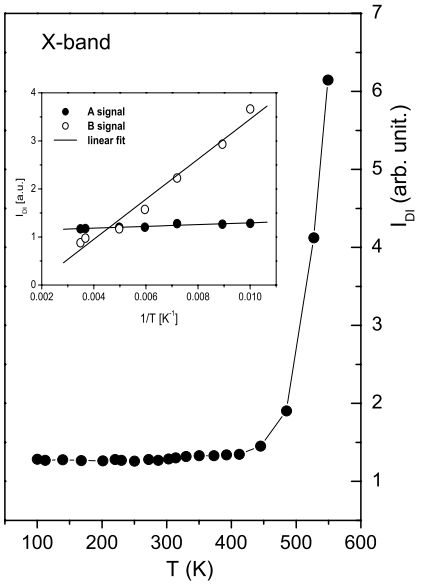

Figure 6. Temperature dependence of the A signal line intensity I_{DI} for Alq_3 fraction 3 as synthesized. The inset shows the temperature dependence of $1/I_{DI}$ for both A and B signals in the region 110–290 K.

Table 1. Room temperature EPR parameters of the A and B signals in sublimated solid Alq_3.

Sample fractions	$g_{eff}^{(A)}$ signal	$g_{eff}^{(B)}$ signal	$\Delta B_{pp}^{(A)}$ (mT)
I	2.00_2	—	1.17
II	1.99_8	—	1.51
III	1.99_8	—	1.48
IV	1.99_8	4.32_2	1.46
V	2.00_1	4.33_7	1.17
VI	2.00_2	4.34_1	1.20

with a rather narrow linewidth, has a particular nature; its integral intensity and linewidth are not temperature dependent from 20 K to high temperature— $T \sim 440$ K for fraction 3 or $T \sim 390$ K for fractions 1 and 2—when a fast increase of I_{DI} appears. Such behaviour is seen in figure 6. A slow recovery of the samples at room temperature is observed. The section of the plot not dependent on temperature suggests that this signal could be associated with delocalized unpaired electrons. So far we cannot explain the fast increase of the intensity, but note that all samples were measured in a sealed quartz tube to avoid the influence of moisture or oxygen.

Interesting results were obtained from irradiated samples. It is well known that irradiation with heavily ionizing radiation provides information about the strength and stability of molecular bonding. Under room temperature irradiation in accelerated electron beams of 6 MeV energy, with a dose of 10 kGy, we observed an increase of the signal A line intensity by a factor of 10 (times). Similar behaviour, with a smaller increase of intensity, was communicated in [17] for γ-irradiated commercial Alq_3. In our case, the largest effect was observed for fraction 2, and the smallest one for fraction 3. Signal B remained unchanged, as seen in

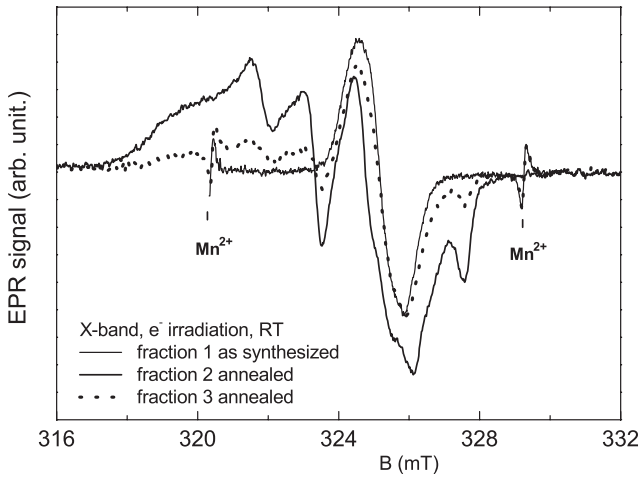

Figure 7. X-band room temperature EPR spectra of e^--irradiated annealed Alq_3 fractions (30 mg of each fraction). Lines 3 and 4 of the Mn^{2+}:MgO field marker are shown.

figure 5(a), proving that it is not associated with any broken chemical bond. On the other hand, new free radical species appear under electron (or γ-) irradiation of annealed fractions 2 and 3. Examples of room temperature EPR spectra are plotted in figure 7. A hyperfine structure due to the interactions with N and H nuclei was observed, partially resolved at low temperatures [25].

3.3. Annealed Alq_3 fractions

Very recently it has been found that by choosing a suitable temperature cycle, in an inert atmosphere, a reversible conversion from Alq_3 fraction 2 or fraction 3 to the high temperature δ-phase of fraction 1 is possible [23, 26]. As the temperature has a significant influence on the formation of these fractions, we made measurements on some selected Alq_3 samples, annealed at different temperatures in the interval 390–400 °C, for 2–6 h. The samples were subsequently cooled down slowly to room temperature or were rapidly quenched in liquid nitrogen. Both the X- and Q-band EPR spectra of these samples are clearly different as compared to the spectra recorded for the material taken from the glass tube; new paramagnetic defect centres are formed, spread over a 1.5 T magnetic field range. Generally, their spectrum intensity increases on lowering the temperature, and the ratio of different lines depends on the annealing temperature and the initial nature of the fraction. Typical X- and Q-band EPR powder-like spectra are presented in figure 8(a); the low temperature dependence of the Q-band spectra, in the field region 1100–1350 mT, is shown in figure 8(b), and the temperature dependence of a high field line intensity of this region is plotted in figure 8(c). The measured sample was selected from fraction 3, which was annealed at 390 °C for 6 h and slowly cooled down to room temperature. The features of the observed EPR lines, as well as their intensity temperature dependence, are indicative of systems with $S \geqslant 1$ electron spin states; these lines are, therefore, attributed to localized quartet and triplet defect paramagnetic centres with low symmetry zero-field splitting tensors. In addition we also observed the expected low field forbidden transitions $\Delta M_S = \pm 2$ and ± 3, which support the assumptions made. This assignment is also corroborated by the observation of a relatively large amplitude of the $\Delta M_S = \pm 2$ line in the X-band spectrum shown in figure 8(a).

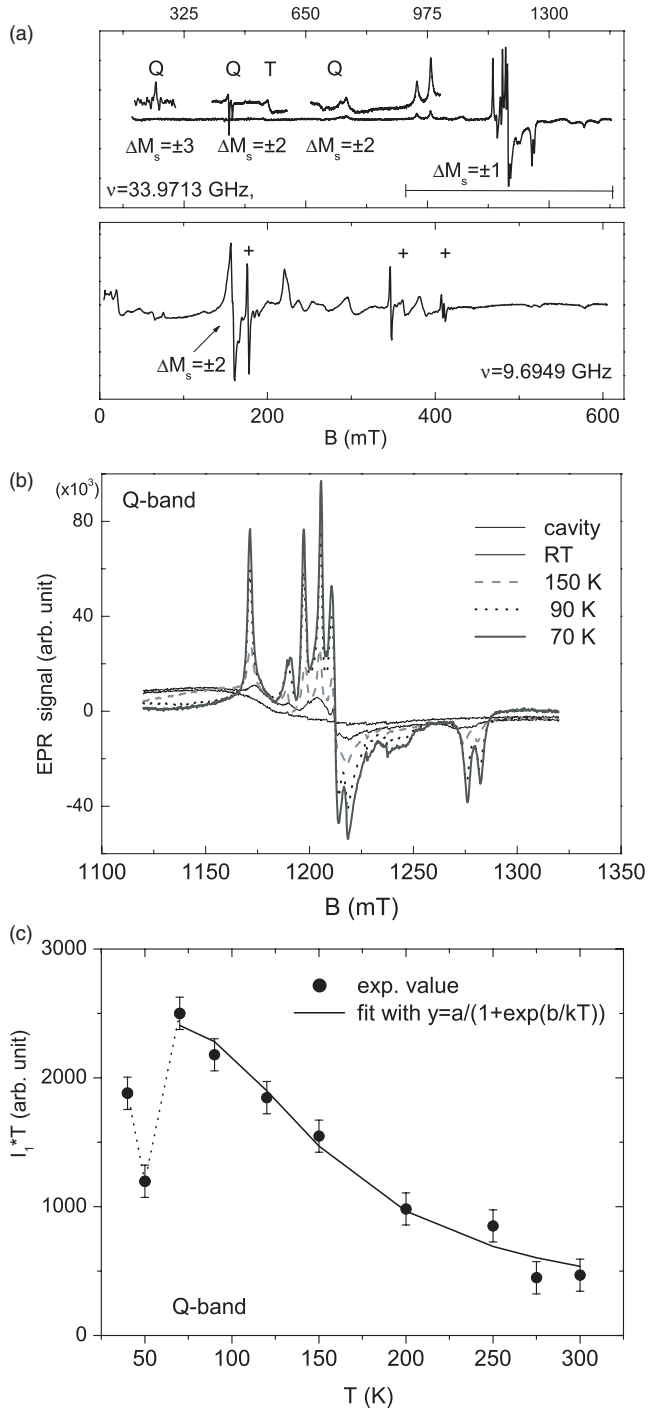

Figure 8. Typical X- and Q-band spectra of an annealed Alq_3 fraction recorded at 50 K (a), and at different temperatures in the Q band for the central part of the spectrum, where $\Delta M_s = \pm 1$ transitions are mainly observed (b). Temperature dependence in the Q band of a $\Delta M_s = 1$ quartet line intensity I_1 at high field, multiplied by T (c). The (+) marked lines in (a) belong to the EPR cavity. Forbidden transitions of quartets and triplets are marked with Q and T, respectively.

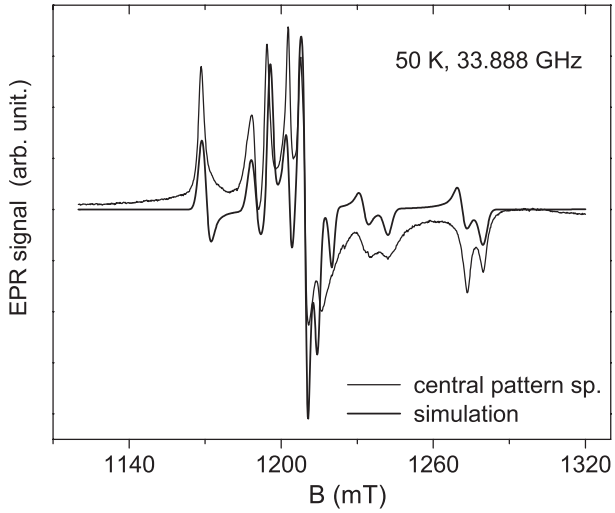

Figure 9. Simulation of the central pattern $\Delta M_s = 1$ spectrum, recorded in the Q band at 50 K. A Gaussian line was used with $\Delta B = 2.5$ mT.

The EPR spectra are fully described by the following spin Hamiltonian (SH) appropriate to $S \geqslant 1$, with the usual notation [27]:

$$\mathcal{H} = D[S_z^2 - (1/3)S^2] + E(S_x^2 - S_y^2) + \mu_B \mathbf{B} \cdot \underline{g} \cdot \mathbf{S}. \tag{1}$$

The g tensor values and corresponding fine-structure splitting D and E parameters were obtained by using the simulation/fit SIM program [28]. Figure 9 shows the simulation of the Q-band EPR central pattern of the spectrum at 50 K. This spectrum consists of the overlapping of different defect centres with $S = 1/2$, 1, and $3/2$. The most important lines, with their relative intensities dependent on the annealing temperature, belong to two quartets randomly oriented. The D and E parameters of these quartets are given in table 2. The SH parameters obtained for the other simulated centres are $g_{iso} = 2.004$, $\Delta B = 1.2$ mT, for a doublet centre, and $|D| = 135\ G$, $|E| = 20\ G$, $g_{iso} = 2.006$ for a triplet centre. Another interesting feature of our EPR data results from the temperature dependence of an annealed Alq_3 fraction suddenly quenched to 77 K. When measuring, for instance, a sample from fraction 2 annealed at 400 °C for 2 h, we observed a drastic change in the EPR spectrum after quenching treatment. The central lines characteristic of quartet and triplet centres disappear and a very strong line appears instead, having an orthorhombic g tensor with the principal values $g_1 = 2.0066$, $g_2 = 2.0042$, $g_2 = 2.0016$; see the inset of figure 10. The intensity of this signal was calibrated with a DPPH probe having $(5.32 \pm 0.70) \times 10^{17}$ spins/g by comparing their double integrals. The number of spins resulting is $(4.25 \pm 0.85) \times 10^{19}$ spins/g. From TEM measurements we found that such samples mainly consisted of crystalline γ-Alq_3 phase. In consequence we associated the EPR signal of the sample with this high temperature phase of Alq_3. We note that a similar anisotropic EPR signal, with a less resolved structure and different intensities, is observed for all annealed fractions slowly relaxed. We associate it with the same type of paramagnetic defect centre as was observed in quenched annealed samples. This would mean that the γ-Alq_3 phase is present in all annealed Alq_3 fractions.

A further characteristic that was obtained for this defect centre is the temperature dependence of its EPR intensity. Figure 10 shows the plot of the double integration of the spectrum intensity I_{DI} versus T. From the data that are available so far, this behaviour

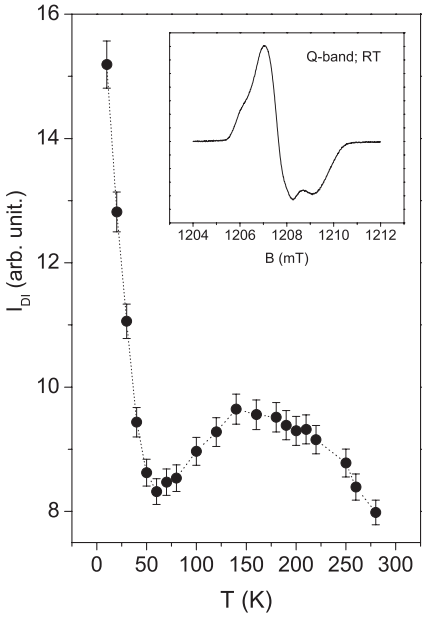

Figure 10. Temperature dependence of the EPR line intensity, I_{DI}, of the γ-Alq_3 phase. The room temperature spectrum in the Q band is given in the inset. The dotted line is a guide for the eye.

Table 2. EPR parameters g and fine-structure D and E values obtained from the spectra simulation.

Defect centre	$\lvert D\rvert$ (cm^{-1})	$\lvert E\rvert$ (cm^{-1})	g
Quartet 1	0.1563	0.0093	2.009; 2.006; 1.996
Quartet 2	0.2310	0.0078	2.006; 2.004; 2.000

cannot be explained. For a conclusive interpretation, further measurements such as ones of the temperature dependence of the magnetic susceptibility are necessary. The sudden change around 55 K shows that a kind of 'phase transition' takes place. We note that thermally stimulated luminescence (TSL) and delayed luminescence measurements [26, 29–32] have shown anomalies at temperatures of $T \sim 60$ K and $T \sim 150$ K, as in our measurements.

4. Discussion and conclusion

For the first time the formation of different paramagnetic centres in non-doped sublimated solid Alq_3, dependent on the preparation, temperature, and annealing, is reported. As such treatments modify the crystallographic structure of the material, we correlate these modifications with the EPR spectra and tentatively propose possible models for the observed paramagnetic centres. For samples as synthesized (obtained by sublimation in a temperature gradient), two different signals are observed: signal A in the region of $g \sim 2$, and signal B in the region of $g \sim 4$. Their intensities have different temperature dependences (see the inset in figure 6), demonstrating their different natures. The intensity I_{DI} of signal A is temperature independent from about 400 K down to low temperatures, even lower than 100 K. Such a paramagnetic centre might be associated with quasi-free electrons, which, like free electrons in metals, show a temperature-independent Pauli magnetism. On the basis of just the EPR data,

it is hard to propose an appropriate model for them. They might be associated with defects in Alq_3 units, having one electron in a delocalized orbital which overlaps with the corresponding orbitals of other defects. The width of the narrow line, with the g value close to $g_e = 2.0023$, sustains such a hypothesis. The concentration of these defect centres is largest for the most strained fraction (green fraction 3), making plausible the idea that the Alq_3^- anion can be formed only in strained regions of the lattice. On raising the temperature above 390–440 K, new centres are formed. The DSC data show that in this temperature range no evident structural change takes place [23]. Therefore another mechanism has to be considered to explain the observed increase of the EPR intensity. It could be the thermal excitations of electrons from diamagnetic states to empty delocalized orbitals of the Alq_3 unit. Other mechanisms cannot be ruled out: effects of oxygen and water [32] (even if the samples were treated in sealed quartz tubes they were exposed to air for a short period of time before), or creation of trap sites on some Alq_3 molecules capable of trapping electrons in delocalized orbitals. Evidently, other measurements are necessary for a full understanding of the origin of signal A.

The second signal B, whose intensity is proportional to $1/T$ (see the inset in figure 6) must be associated with a localized paramagnetic centre. Its resonance field suggests a forbidden transition $\Delta M = \pm 2$ of a triplet in the ground state. Taking the g value close to g_e, as in all triplet states, its resonance field is $H_B < H_0/2$, which means rather a large zero-field splitting. Assuming a significant disorder in the matrix, the very anisotropic $\Delta M = \pm 1$ transitions are rather broad and consequently quite weak. The $\Delta M = \pm 2$ spectrum is less sensitive to zero-field splitting fluctuations, so it gives narrower lines. From this line one can obtain the D and E values. The structured line of centre B was fitted with two triplet centres ($S = 1$) having the following fine-structure parameters: $D^{(1)} = 0.115\ \text{cm}^{-1}$, $E^{(1)} = 0.01\ \text{cm}^{-1}$ and $D^{(2)} = 0.135\ \text{cm}^{-1}$, $E^{(2)} = 0.012\ \text{cm}^{-1}$ ($g_{iso} = 2.004$ and a Gaussian line shape with a linewidth of 2.5 mT was used). As we have already said, the ground state of the centre B is a triplet state, so one model could be an Alq_3^{2-} di-anion. The existence of hyperfine interactions with H and even N nuclei is not excluded. ENDOR and ESEEM measurements are necessary to prove this supposition.

The essential changes in the EPR spectra for the annealed samples are related to crystallographic changes in the samples induced by such thermal treatments. As x-ray and electron microscopy diffractions show, the γ- and δ-Alq_3 phases are dominant in annealed samples. Recent studies [5, 15] have shown for these phases that the facial isomer is dominant and stable. This isomer, having a C_3 local symmetry, has a degenerate LUMO orbital associated with a close non-degenerate orbital [20]. It seems very plausible that a tri-anion Alq_3^{-3}, with three electrons in these lowest LUMO orbitals, has two doublet states close to a quartet spin state ($S = 1/2, 3/2$). In the EPR spectra presented in figure 8, the most significant change is the appearance of such a quartet state, with fairly large D and E values. It is clearly seen in the Q band where $D/h\nu \sim 1/10$, so a perturbation treatment is still reasonable. As was already stated, $\Delta M = \pm 2$ and ± 3 transitions confirm its existence. The intensity temperature dependence of this centre (given in figure 8(c)) fitted with $y = a/T(1 + e^{b/kT})$, $b\ (=3J) = -43$ meV, where J is the isotropic exchange coupling constant, shows that the quartet state is lower than the doublet. At low temperatures a kind of *phase transition* around 55 K is observed for all annealed samples. Fast quenching of an annealed sample of fraction 2, from 400 to $-197\,^\circ$C, induces a narrow and very strong EPR signal. TEM measurement data showed that in this sample, microcrystals with γ-Alq_3 structure predominate. The fast quenching forbids the transformation from this high temperature phase to other Alq_3 phases, but leaves the structure with high strains. We assume that only less anisotropic lines can be observed and these could probably correspond either to a mono-anion Alq_3^- or to the doublet state of the tri-anion Alq_3^{-3}.

In conclusion, different paramagnetic centres in microcrystalline Alq_3 fractions, as synthesized and annealed, have been observed and investigated. Their nature, their temperature dependence, as well as the correlation with the crystal structure have been reported for the first time, and possible models have been discussed. Further measurements are required to prove their validity and to confirm the relation to the molecular symmetry, namely the connection to either mer-isomers or fac-isomers of Alq_3.

Acknowledgments

Financial support by SFB 481 is gratefully acknowledged and thanks go to Dr W Bietsch for helpful discussions. In particular we would like to thank Jürgen Gmeiner for preparation of the Alq_3 samples and Professors Dr Wolfgang Brütting and Dr Voicu Grecu for their interest and important recommendations made during the research.

References

[1] Tang C W and Van Slyke S A 1987 *Appl. Phys. Lett.* **51** 913
[2] Brütting W, Berleb W and Mückl A 2001 *Org. Electron.* **2** 1
[3] Masciocchi N and Sironi A 1997 *J. Chem. Soc. Dalton Trans.* 4643
[4] Brinkmann M, Gadret G, Muccini M, Taliani C, Masciocchi N and Sironi A 2000 *J. Am. Chem. Soc.* **122** 5147
Brinkmann M, Gadret G, Muccini M, Taliani C, Masciocchi N and Sironi A 2001 *Synth. Met.* **121** 1499
[5] Cölle M, Dinnebier R E and Brütting W 2002 *Chem. Commun.* **23** 2908
[6] Amati M and Lelj F 2002 *Chem. Phys. Lett.* **358** 144
[7] Kushto G P, Iizumi Y, Kido J and Kafafi Z H 2000 *J. Phys. Chem.* A **104** 3670
[8] Li H, Zhang F, Wang Y and Zheng D 2003 *Mater. Sci. Eng.* B **100** 40
[9] Muccini M, Loi M A, Kenevey K, Zamboni R, Masciocchi N and Sironi A 2004 *Adv. Mater.* **16** 861
[10] Braun M, Gmeiner J, Tzolov M, Cölle M, Meyer F D, Milius W, Hillebrecht H, Wendland O, von Schütz J U and Brütting W 2001 *J. Chem. Phys.* **114** 9625
[11] Halls M D and Aroca R 1998 *Can. J. Chem.* **76** 1730
[12] Espasti A, Brinkman M, Ruoni G and Zamboni R 2002 *Synth. Met.* **127** 247
[13] Cölle M, Forero-Lenger S, Gmeiner J and Brütting W 2003 *Phys. Chem. Chem. Phys.* **5** 2958
[14] Utz M, Chen C, Morton M and Papadimitrakopoulos F 2003 *J. Am. Chem. Soc.* **125** 1371
[15] Utz M, Nandagopal M, Mathai M and Papadimitrakopoulos F 2003 *Appl. Phys. Lett.* **83** 4023
[16] Li G, Kim H, Lane P A and Shinar J 2004 *Phys. Rev.* B **69** 165311
[17] Pode R B, Roy V A L, Gundurao T K and Baldacchini G 2000 *Proc. 10th Int. Workshop on Inorganic and Organic Electroluminescence (Hamamatsu, Japan, Dec. 2000)* p 183
[18] Ravi Kishore V V, Periasamy N, Bhattacharjee B, Ranjan Das, Paulose P L and Narasimhan K L 2003 *Chem. Phys. Lett.* **367** 657
[19] Roy V A L, Pode R B, Gundu Rao T K, Djurišic A B and Baldacchini G 2004 *Mater. Sci. Eng.* B **106** 85
[20] Amati M and Lelj F 2003 *J. Phys. Chem.* A **107** 2560
[21] Zhang J and Frenking G 2004 *J. Phys. Chem.* A **108** 10296
[22] Curioni A, Boero M and Andreoni W 1998 *Chem. Phys. Lett.* **294** 263
[23] Cölle M, Gmeiner J, Milius W, Hillebrecht H and Brütting W 2003 *Adv. Funct. Mater.* **13** 108
[24] Ghica C, Grecu M N, Gmeiner J and Grecu V V 2005 *J. Optoelectron. Adv. Mater.* at press
[25] Mirea A, Grecu M N, Gmeiner J and Grecu V V 2005 to be published
[26] Cölle M and Brütting W 2004 *Phys. Status Solidi* a **201** 1095
[27] Weil J A, Bolton J R and Wertz J E 1994 Electron paramagnetic resonance *Elementary Theory and Practical Applications* (New York: Wiley–Interscience)
[28] Jacobsen C J H, Pedersen E, Villadsen J and Weihe H 1993 *Inorg. Chem.* **32** 1216
[29] Forsythe E W, Morton D C, Tang C W and Gao Y 1998 *Appl. Phys. Lett.* **73** 1457
[30] Cölle M, Gärditz C and Braun M 2004 *J. Appl. Phys.* **96** 6133
[31] Cölle M and Gärditz C 2004 *J. Lumin.* **110** 200
[32] Kwong K Y, Djurišić A B, Choy W C H, Li D, Xie M H, Chan W K, Cheah K W, Lai P T and Chui P C 2005 *Mater. Sci. Eng.* B **116** 75